



US006222778B1

(12) **United States Patent**  
**Ahn et al.**

(10) **Patent No.:** **US 6,222,778 B1**  
(45) **Date of Patent:** **Apr. 24, 2001**

(54) **SINGLE ELECTRON MOSFET MEMORY DEVICE AND METHOD**

(75) Inventors: **Kie Ahn**, Chappaqua, NY (US);  
**Leonard Forbes**, Corvallis, OR (US)

(73) Assignee: **Micron Technology, Inc.**, Boise, ID (US)

(\*) Notice: Subject to any disclaimer, the term of this patent is extended or adjusted under 35 U.S.C. 154(b) by 0 days.

(21) Appl. No.: **09/619,265**

(22) Filed: **Jul. 19, 2000**

**Related U.S. Application Data**

(62) Division of application No. 09/140,624, filed on Aug. 26, 1998, now Pat. No. 6,125,062.

(51) **Int. Cl.**<sup>7</sup> ..... **G11C 7/00**

(52) **U.S. Cl.** ..... **365/189.07; 365/185.29**

(58) **Field of Search** ..... **365/189.07, 185.29, 365/185.18; 257/314, 315, 321**

(56) **References Cited**

**U.S. PATENT DOCUMENTS**

3,675,090	*	7/1972	Neale	257/3
4,939,559		7/1990	DiMaria et al.	257/321
5,731,598		3/1998	Kado et al.	257/30
5,740,104		4/1998	Forbes	365/185.03
5,952,692		9/1999	Nakazato et al.	257/321

**OTHER PUBLICATIONS**

Lingjie Guo et al., "A room-temperature silicon single-electron metal-oxide-semiconductor memory with nanoscale floating-gate and ultranarrow channel," *Appl. Phys. Lett.* 70(7):850-852, Feb. 1997.

Lingjie Guo et al., "Fabrication and characterization of room temperature silicon single electron memory," *J. Vac. Sci. Technol. B*, 15(6):2840-2843, Nov./Dec. 1997.

Rodrigo Martins et al., "Transport properties of doped silicon oxycarbide microcrystalline films produced by spatial separation techniques," *Solar Energy Materials and Solar Cells*, 41/42:493-517, 1996.

Anri Nakajima et al., "Room Temperature Operation of Si Single-Electron Memory with Self-Aligned Floating Dot Gate," *IEDM 96*, pp. 952-954, 1996.

Anri Nakajima et al., "Room Temperature Operation of Si Single-Electronic Memory with Self-Aligned Floating Dot Gate," *Appl. Phys. Lett.* (70)13:1742-1744, Mar., 1997.

Anri Nakajima et al., "Si single electron tunneling transistor with nanoscale floating dot stacked on a Coulomb island by self-aligned process," *Appl. Phys. Lett.* 71(3):353-355, Jul. 1997.

Sandip Tiwari et al., "Single charge and confinement effects in nano-crystal memories," *Appl. Phys. Lett.* 69(9):1232-1234, Aug. 1996.

(List continued on next page.)

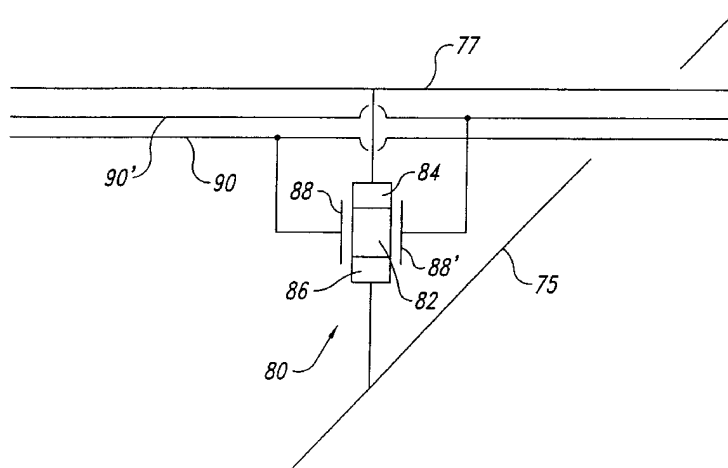
*Primary Examiner*—Amir Zarabian

(74) *Attorney, Agent, or Firm*—Dorsey & Whitney LLP

(57) **ABSTRACT**

A memory device and related methods are described. The memory device includes a plurality of cells, each cell including a MOSFET having a source coupled to a first end of a channel, a drain coupled to a second end of the channel, a gate formed on a gate insulator and extending from the source to the drain and a plurality of conductive islands, each surrounded by an insulator, formed in the channel. The islands have a maximum dimension of three nanometers. The island surrounding insulator is formed in a pore extending into the channel. As a result, the memory cells are able to provide consistent, externally observable changes in response to the presence or absence of a single electron on the island.

**7 Claims, 12 Drawing Sheets**



## OTHER PUBLICATIONS

- Hussein I. Hanafi, "Fast and Long Retention-Time Nano-Crystal Memory," *IEEE Transactions on Electron Devices* 43(9):1553-1558, Sep. 1996.
- G. Craciun et al., "On the morphology of porous silicon layers obtained by electrochemical method," *1995 International Semiconductor Conference*, 18<sup>th</sup> Edition, pp. 331-334, Oct. 1995.
- Tomoyuki Ishii et al., "A 3-D Single-Electron-Memory Cell Structure with  $2F^2$  per bit," *IEDM*, pp. 924-926, 1997.
- K. Yano et al., "Single-Electron-Memory Integrated Circuit for Giga-to-Tera Bit Storage," *ISSCC Digest of Technical Papers*, pp. 266-267, Feb. 1996.
- K. Yano et al., "A 128Mb Early Prototype for Gigascale Single-Electron Memories," *ISSCC Digest of Technical Papers*, pp. 344-345, Feb. 1998.
- Haroon Ahmed and Kazuo Nakazato, "Single-electron devices," *Microelectronic Engineering* 32:297-315, 1996.
- Haroon Ahmed, "Single electron electronics: Challenge for nanofabrication," *J. Vac. Sci Technol. B.* 15(6):2101-2108, Nov./Dec. 1997.
- Tomoyuki Ishii, "Verify: Key to the Stable Single-Electron-Memory Operation," *IEDM*, pp. 171-174, 1997.
- Valery M. Dubin, "Formation mechanism of porous silicon layers obtained by anodization of monocrystalline n-type silicon in HF solutions," *Surface Science* 274:82-92, 1992.
- Jian-Shing Luo and Wen-Tai Lin, "Localized epitaxial growth of hexagonal and cubic SiC films on Si by vacuum annealing," *Appl. Phys. Lett.* 69(7):916-918, Aug. 1996.
- Donato Montanari et al., "Novel Level-Identifying Circuit for Flash Multilevel Memories," *IEEE Journal of Solid-State Circuits* 35(7):1090-1095, Jul. 1998.
- Nae-In Lee et al., "Highly Reliable Polysilicon Oxide Grown by Electron Cyclotron Resonance Nitrous Oxide Plasma," *IEEE Electron Device Letters* 18(10):486-488, Oct. 1997.
- Masato Tarakomori and Hideaki Ikoma, "Low-Temperature Si Oxidation Using Inductively Coupled Oxygen-Argon Mixed Plasma," *Jpn. J. Appl. Phys.* 36:5409-5415, 1997.
- Jin-Woo Lee et al., "Oxidation of Silicon Using Electron Cyclotron Resonance Nitrous Oxide Plasma and Its Application to Polycrystalline Silicon Thin Film Transistors," *Journal of the Electrochemical Society* 144(9):3283-3287, Sep. 1997.
- W.S. Park et al., "Growth of polycrystalline silicon at low temperature on hydrogenated microcrystalline silicon seed layer," *Mat. Res. Soc. Symp. Proc.* 467:403-408, 1997.
- T. Nishimiya et al., "Novel Plasma Control Method in PECVD for Preparing Microcrystalline Silicon," *Mat. Res. Soc. Symp. Proc.* 467:397-401, 1997.
- Constantin Papadas et al., "Modeling of the Intrinsic Retention Characteristics of FLOTOX EEPROM Cells Under Elevated Temperature Conditions," *IEEE Transactions on Electron Devices* 42(4):678-682, Apr. 1995.
- Brian Dipert and Lou Hebert, "Flash memory goes mainstream," *IEEE Spectrum*, pp. 48-52, Oct. 1993.
- Joao Pedro Conde et al., "Amorphous and Microcrystalline Silicon Deposited by Low-Power Electron-Cyclotron Resonance Plasma-Enhanced Chemical-Vapor Deposition," *Jpn. J. Appl. Phys.* 36:38-49, Jan. 1997.
- D.M. Wolfe et al., "Low-Temperature (450° C) Poly-Si Thin Film Deposition on SiO<sub>2</sub> and Glass Using a Microcrystalline-Si Seed Layer," *Mat. Res. Soc. Symp. Proc.* 472:427-432, 1997.
- Yasuo Tarui, "Flash Memory Features Simple Structure, Superior Integration," *JEE* 30:84-87, Sep. 1993.

\* cited by examiner

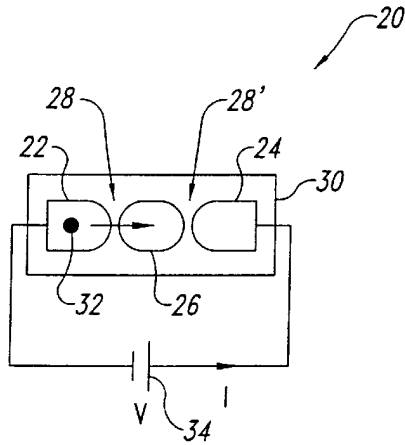


*Fig. 1A*  
(PRIOR ART)

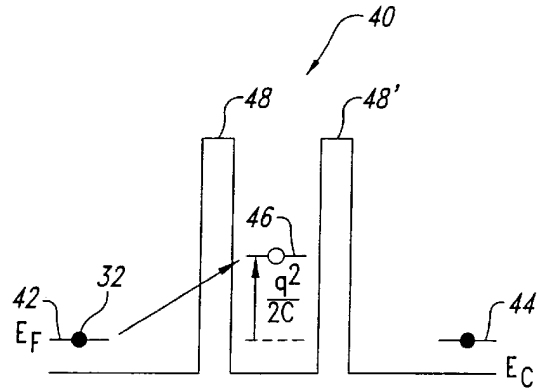


*Fig. 1B*  
(PRIOR ART)

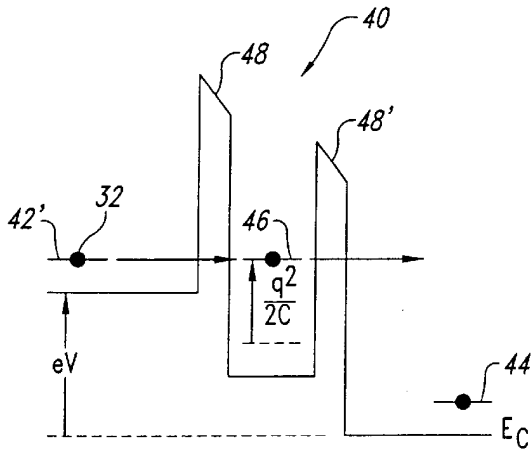


*Fig. 1C*  
(PRIOR ART)

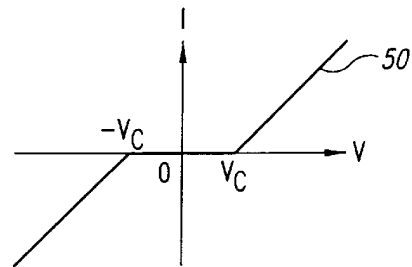


*Fig. 1D*  
(PRIOR ART)

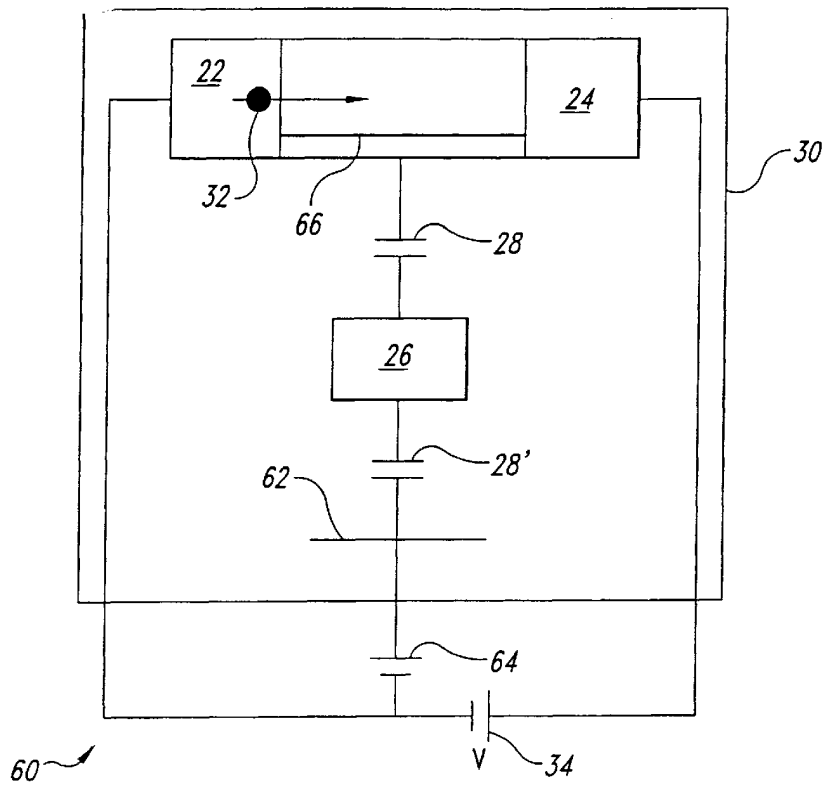


*Fig. 2*  
*(PRIOR ART)*

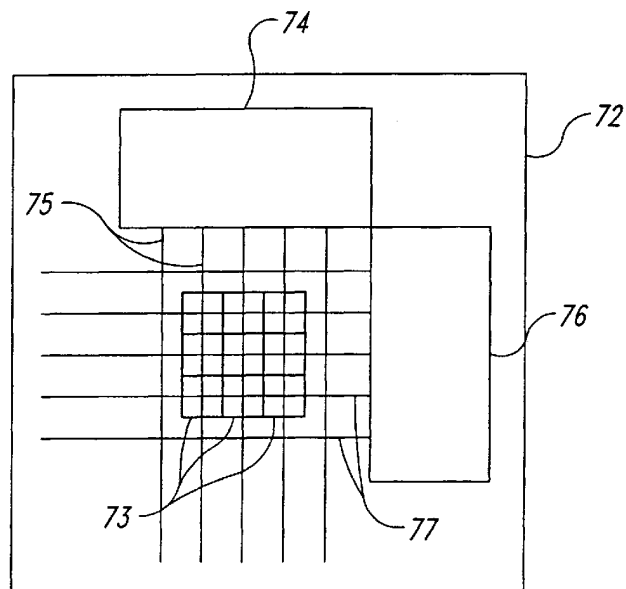


*Fig. 3A*

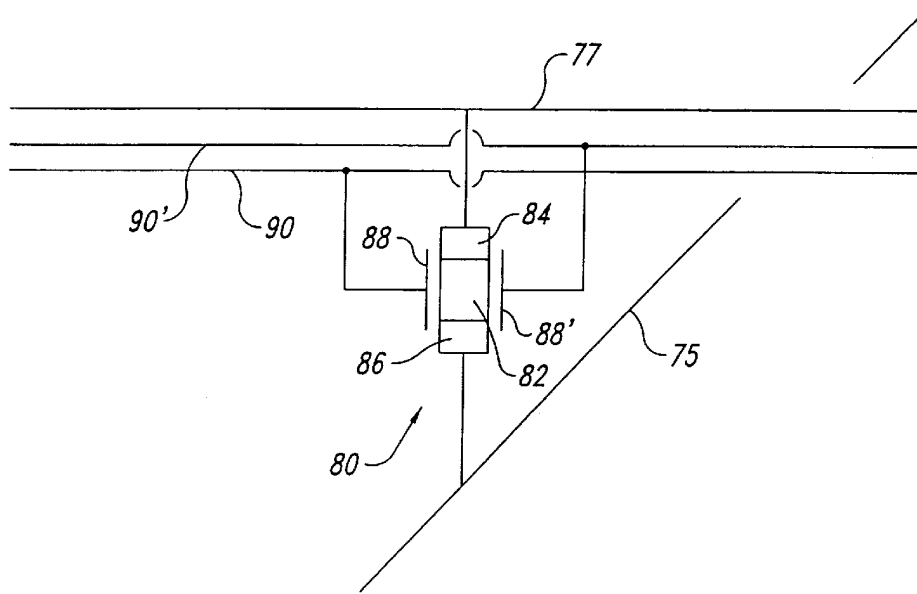


Fig. 3B

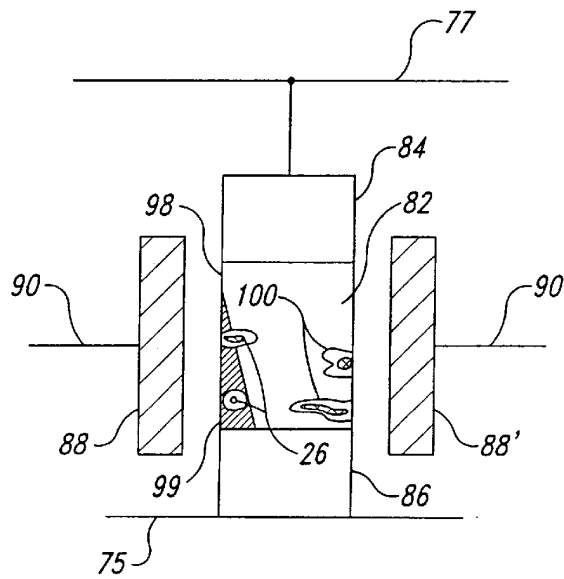


Fig. 3C

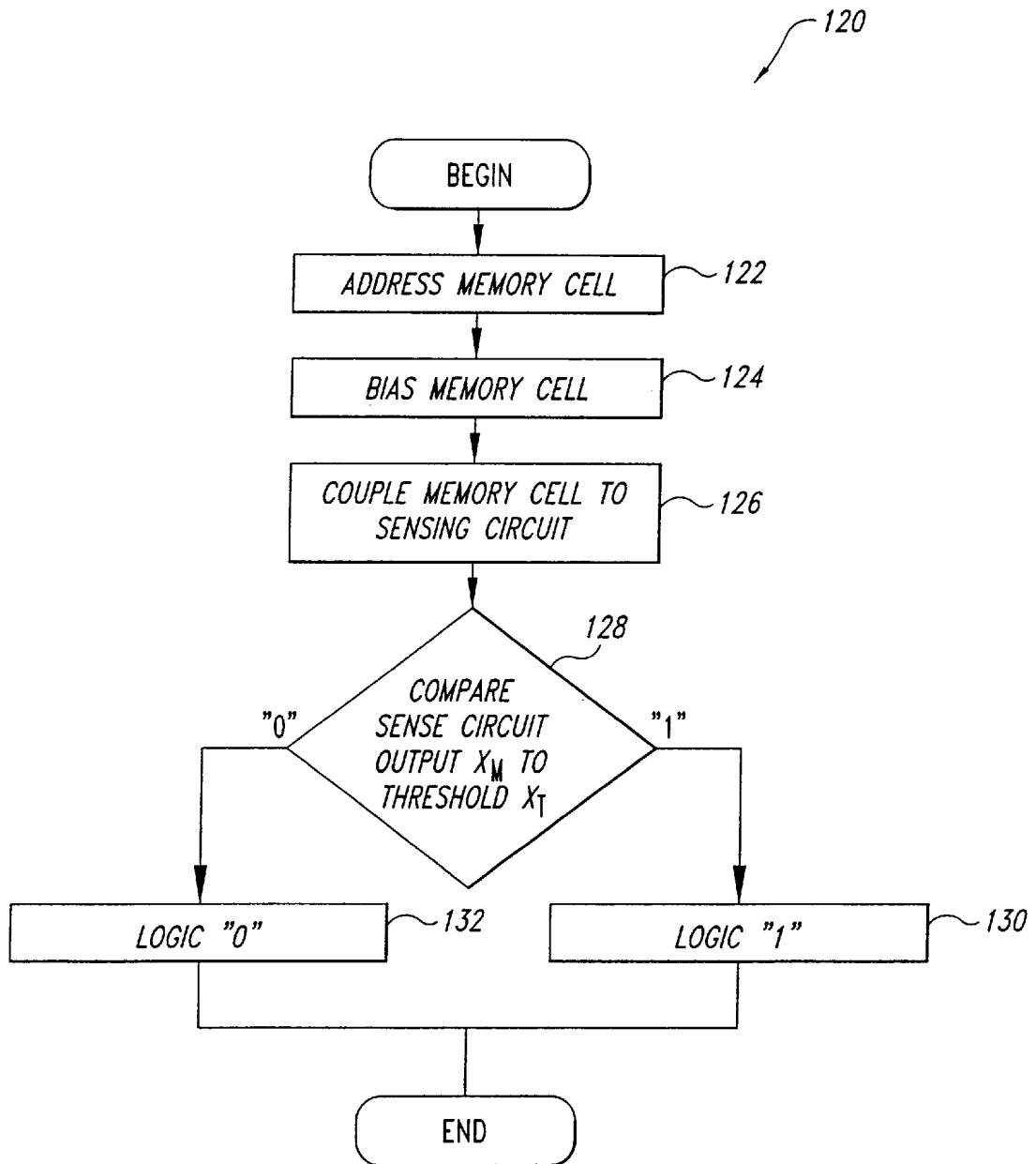


Fig. 4

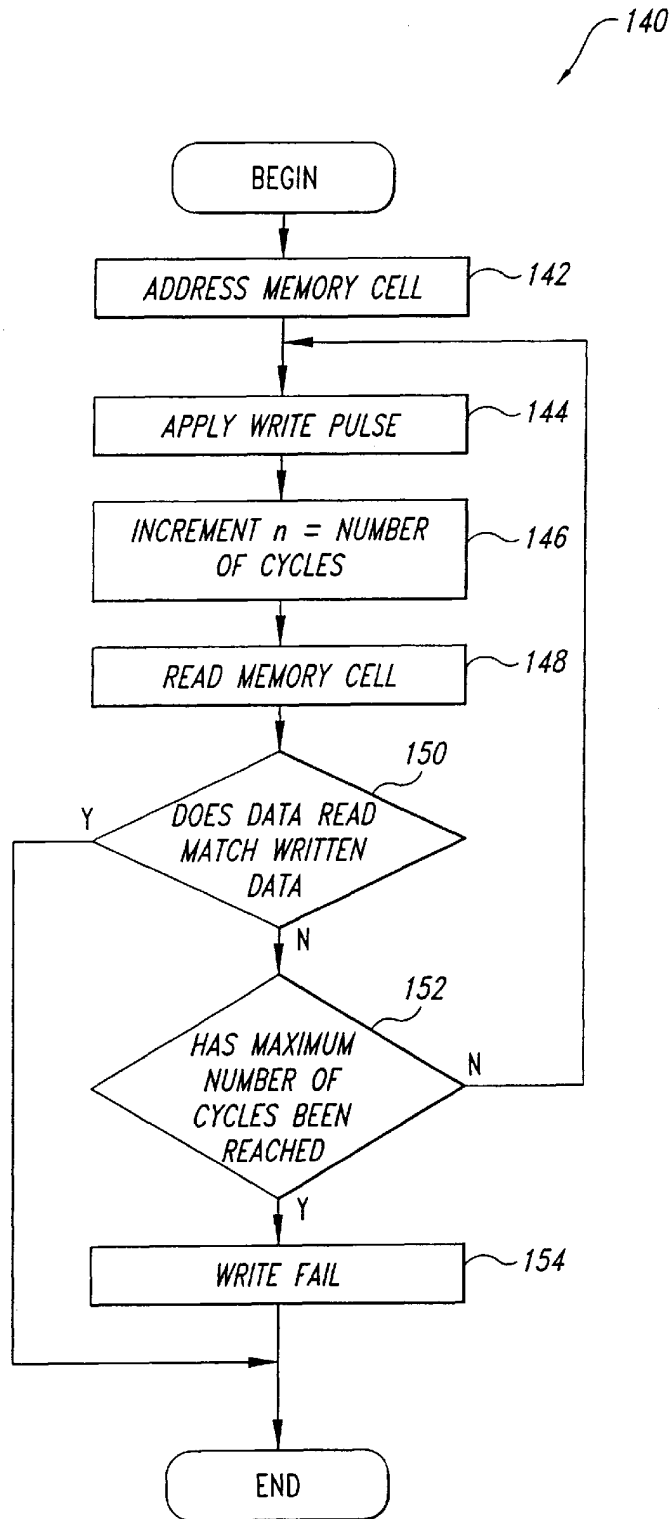


Fig. 5

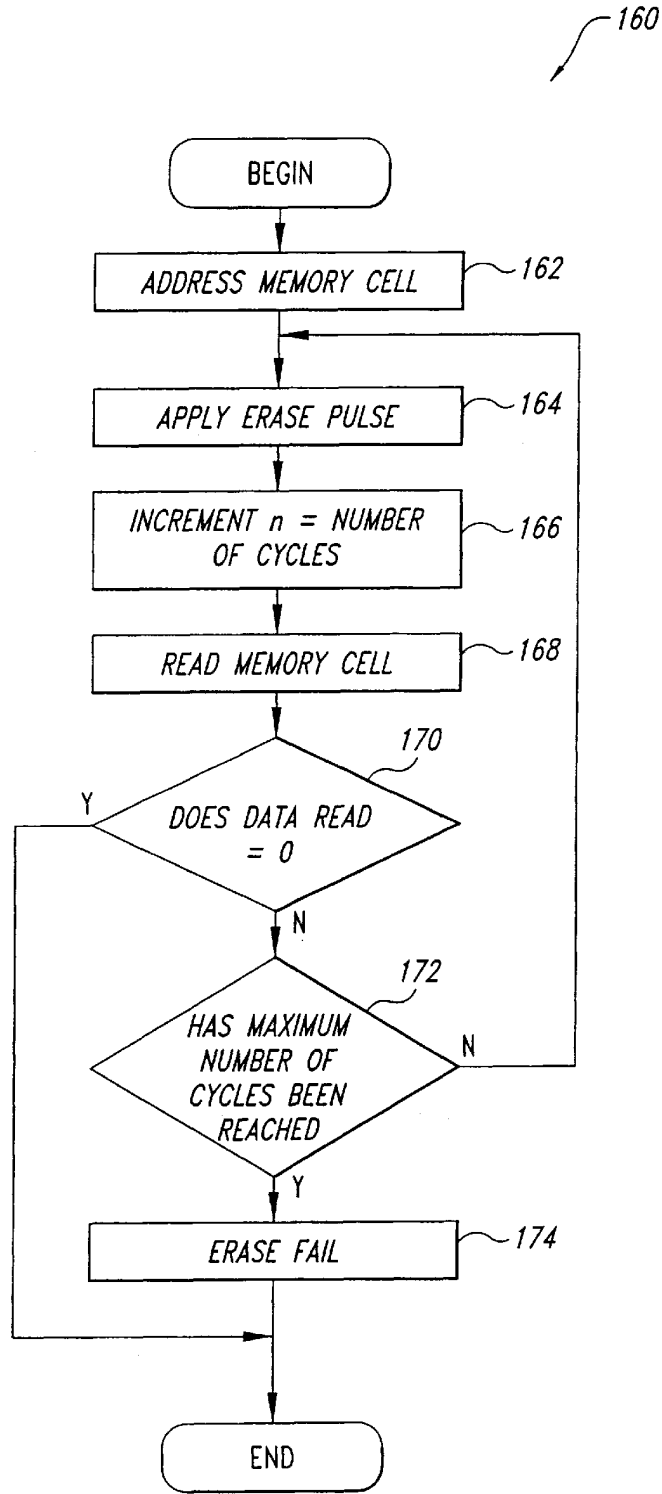


Fig. 6

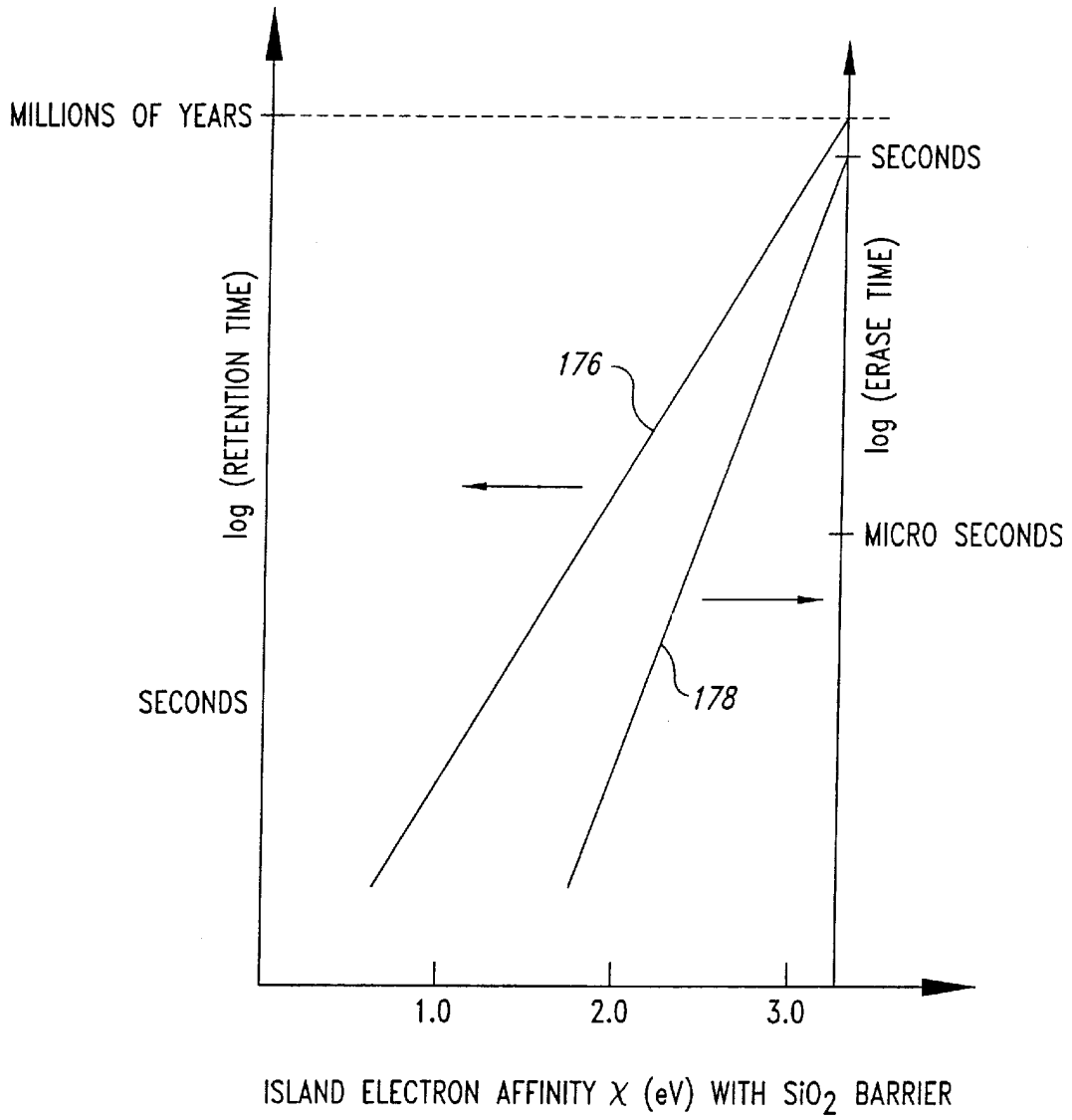
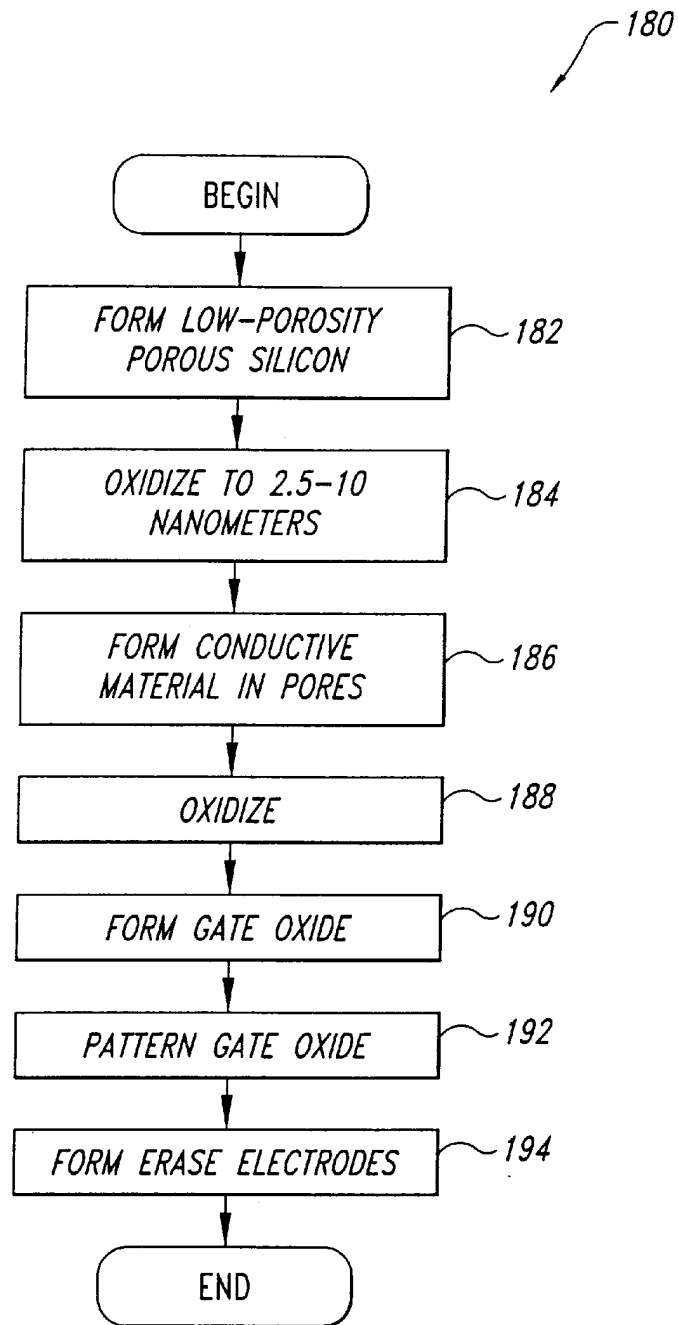
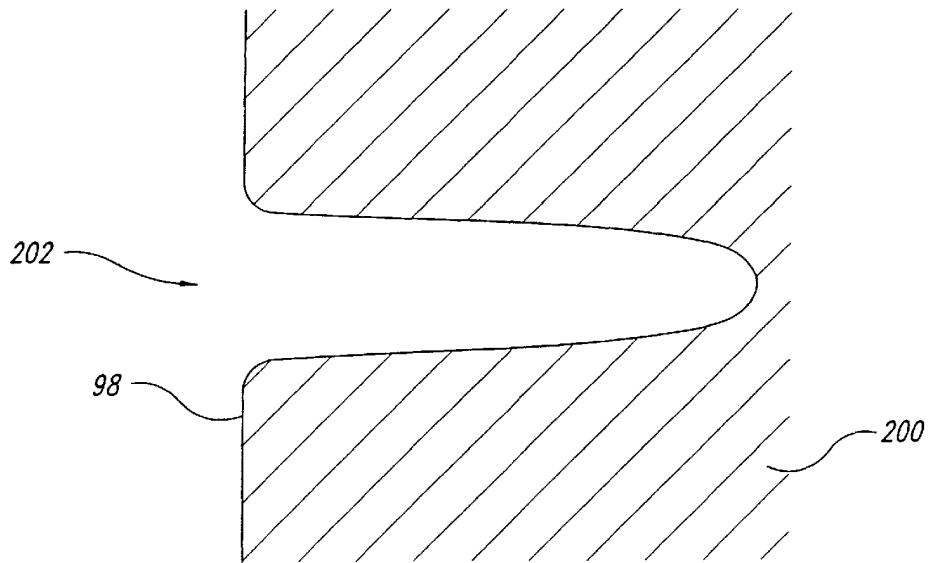


Fig. 7



*Fig. 8*



*Fig. 9A*

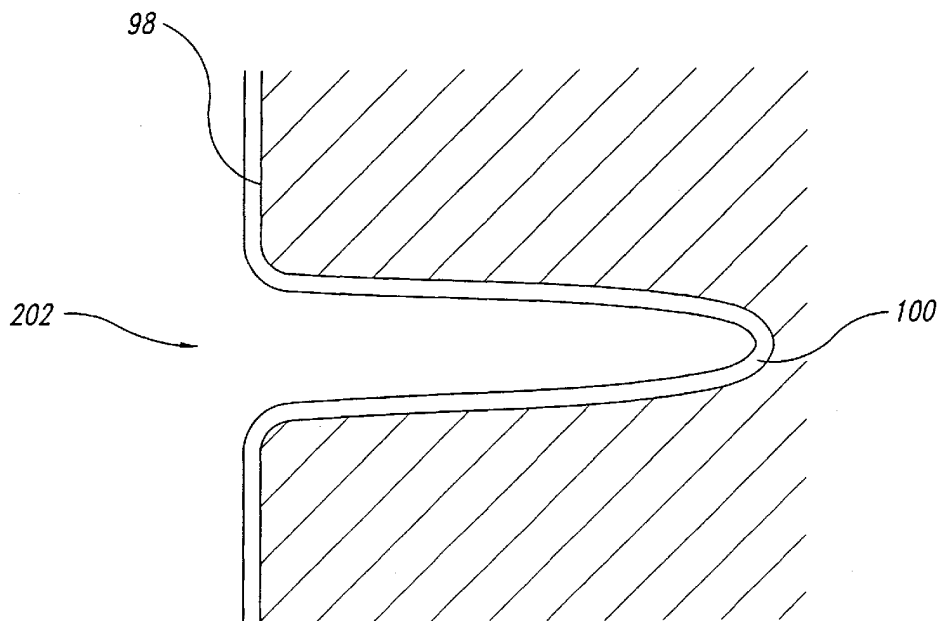


*Fig. 9B*

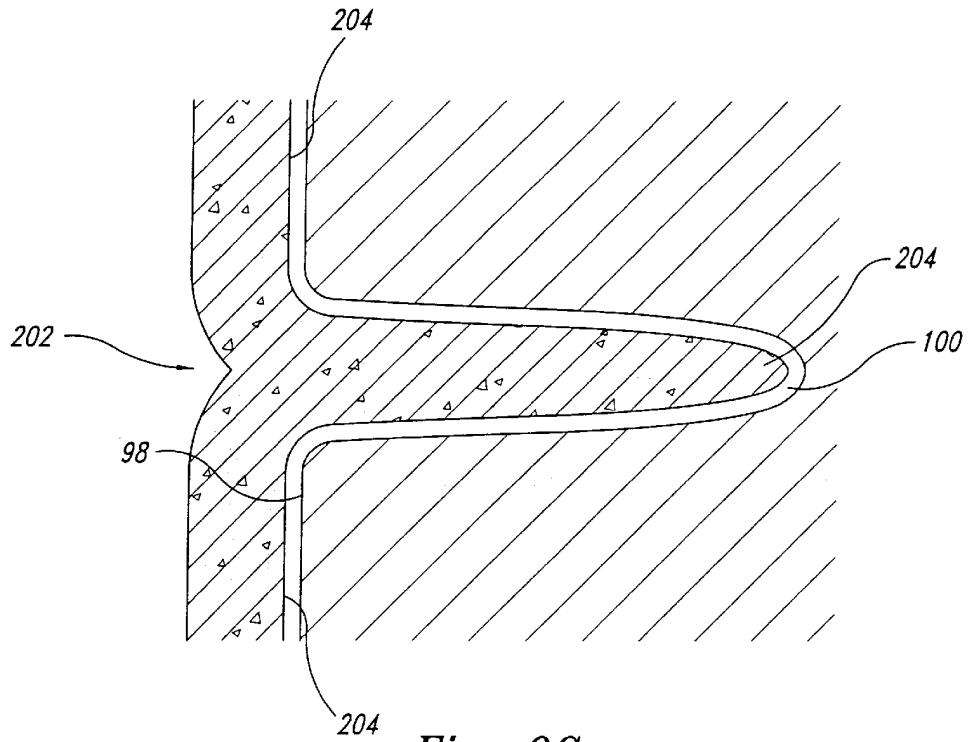


*Fig. 9C*

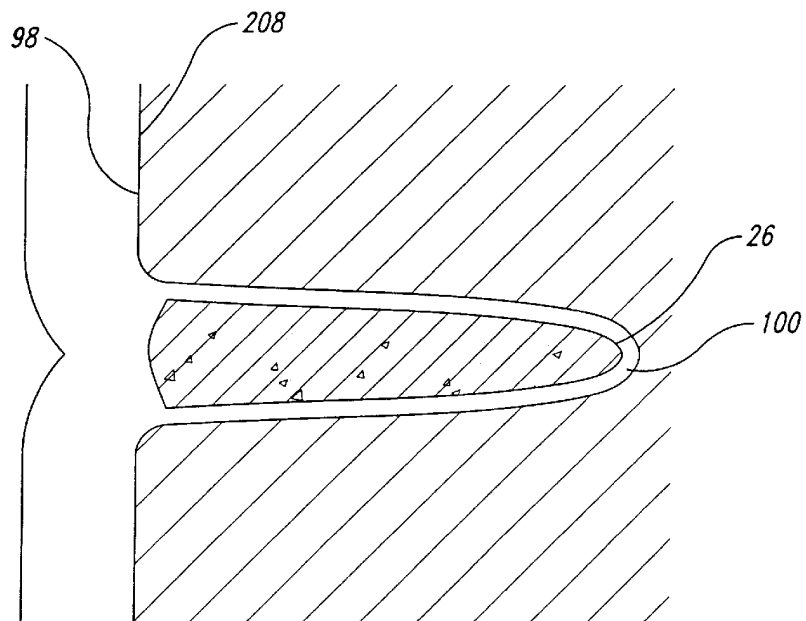


*Fig. 9D*

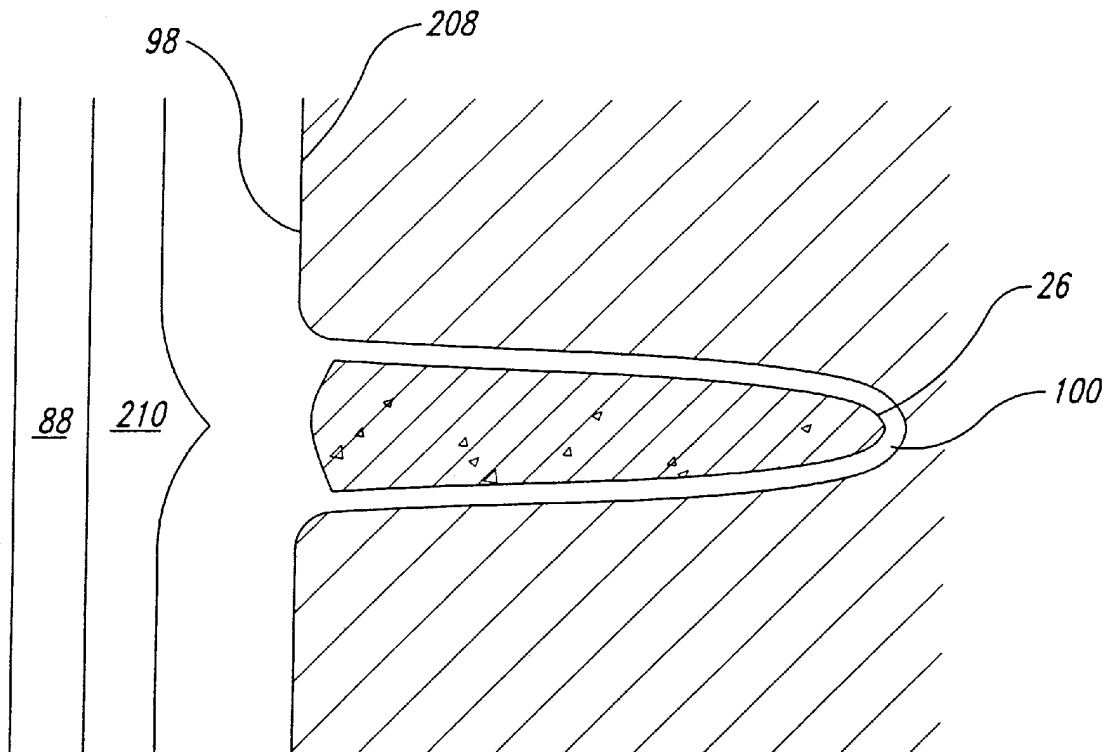


*Fig. 9E*

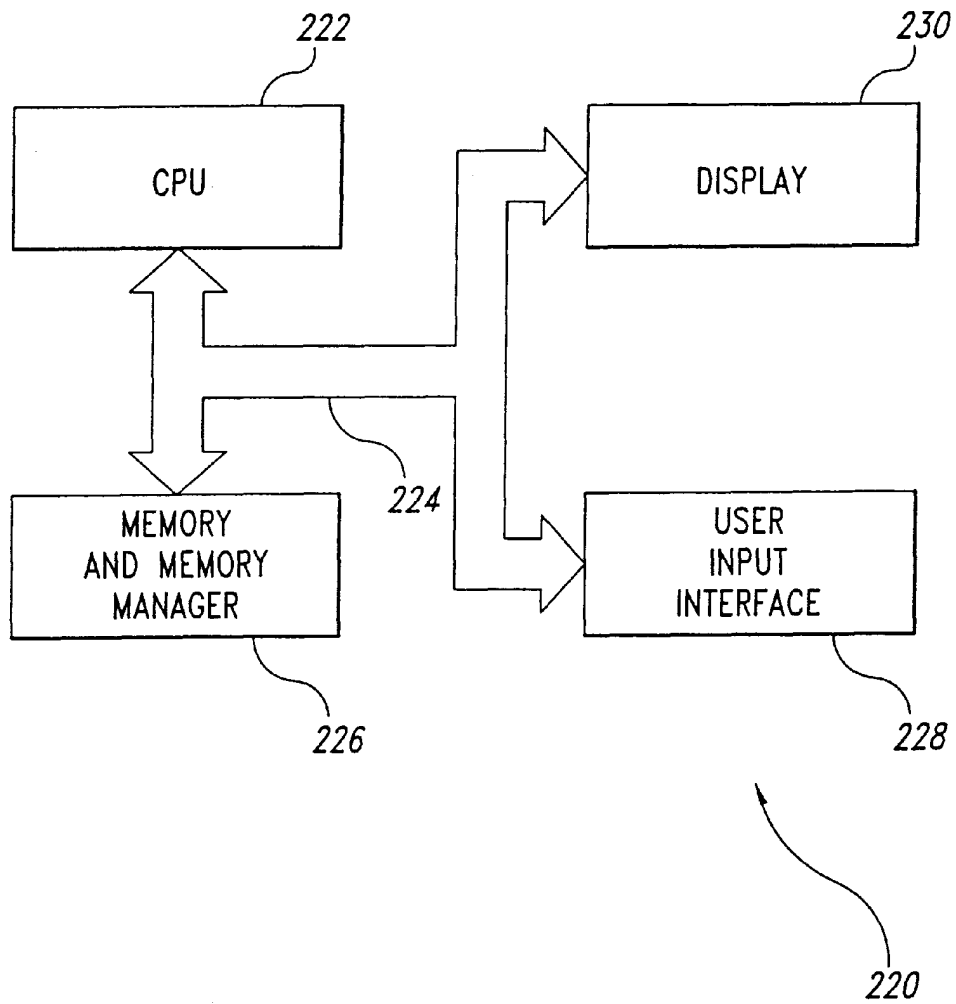


Fig. 10

## SINGLE ELECTRON MOSFET MEMORY DEVICE AND METHOD

### CROSS-REFERENCE TO RELATED APPLICATION

This application is a divisional of pending U.S. patent application No. 09,140,624, filed Aug. 26, 1998 U.S. Pat. No. 6,125,062.

### TECHNICAL FIELD

This invention relates to integrated circuit memory devices, and, more particularly, to a method and apparatus for providing high density, high storage capacity, low power, nonvolatile memory devices.

### BACKGROUND OF THE INVENTION

Single electron devices, and particularly single electron memory cells, are presently of great interest, due to potential advantages in memory cell size and power dissipation, compared to memory technologies currently in use. As used herein, the term "single electron device" refers to an electronic device capable of providing a repeatable and measurable response to the presence or absence of a single electron.

As device sizes have shrunk over the last several decades, the number of electrons contributing to the drain current in field effect transistors ("FETs") used in memory devices has correspondingly decreased. Extrapolation from these trends suggests that in another decade, FETs will have drain currents including as few as ten electrons at a time. When so few electrons contribute to a current and therefore to a signal, normal fluctuations in the number of electrons present in a volume of semiconductor material can lead to uncertainty or error in the signal that the current represents.

Memories using single electron memory cells provide certainty in numbers of electrons representing data in a memory cell and therefore help to avoid problems due to fluctuations in the number of electrons that are present in a transistor at one time. Memory cells employing single electron transistors are also extremely simple and can be quite small. For example, a memory structure employing vertically stacked cells to provide an area per bit of 0.145 micrometers squared is described in "A 3-D Single-Electron-Memory Cell Structure with  $2F^2$  per bit" by T. Ishii et al. (IEDM 97), pp. 924-926.

The combination of size, power requirements and simplicity make single electron structures promising candidates for very high capacity memory integrated circuits. This is discussed in more detail "Single-Electron-Memory Integrated Circuit for Giga-to-Tera Bit Storage" by K. Yano et al., 1996 Intl. Solid State Circuits Conf. (Feb. 9, 1996) pp. 226-267 and "A 128 Mb Early Prototype for Gigascale Single-Electron Memories" by K. Yano et al., 1998 Intl. Solid State Circuits Conf. (Feb. 7, 1998), pp. 344-345.

FIG. 1A is a simplified schematic diagram of a typical two-terminal single electron device **20**, in accordance with the prior art. The single electron device **20** includes first **22** and **24** electrodes and an island **26** formed from conductive material, which may be semiconductor material, as discussed in U.S. Pat. No. 5,731,598, entitled "Single Electron Tunnel Device And Method For Fabricating The Same" issued to H. Kado et al. (Mar. 24, 1998). The first **22** and second **24** electrodes are each separated from the island **26** by small insulating gaps **28**, **28'**. The first **22** and second **24** electrodes, the island **26** and the gaps **28**, **28'** are all collectively mounted on an insulating substrate **30** or are

surrounded by an insulator. The gaps **28**, **28'** may be formed of any insulating material must be small enough to allow conduction band electrons **32** (hereinafter "electrons") to tunnel through them in response to a voltage  $V$  coupled across the first **22** and second **24** electrodes. The voltage  $V$  is provided by an external source, represented in FIG. 1A by a battery **34**.

A first condition for trapping one or more electrons **32** on the island **26** is that the resistance  $R$  between the island **26** and other structures on the substrate **30** must be greater than a quantum resistance  $R_k$  as is discussed, for example, in "Single-electron devices" by H. Ahmed et al., *Microelectronic Engineering* 32 (1996), pp. 297-315, and "Single electron electronics: Challenge for nanofabrication" by H. Ahmed, *J. Vac. Sci. Technol. B* 15(6) (November/December 1997) pp. 2101-2108. When the first **22** and second **24** electrodes and the island **26** are mounted on the insulating substrate **30** and are surrounded by an insulator such as air, the primary resistance  $R$  between the island **26** and any other structure is set by tunneling resistances  $R_t$  associated with the gaps **28**, **28'** separating the island **26** from the first **22** and second **24** electrodes. The quantum resistance  $R_k$  equals  $h/q^2$ , or about 26 k $\Omega$ , where  $h$  is Planck's constant and  $q$  represents the charge of a single electron. This first condition will be satisfied for all of the examples considered herein but is included for completeness sake.

A second condition is that allowed states for these electrons **32** must be separated from a conduction band edge  $E_C$  by an "electron charging energy" that is given as  $q^2/2C$ , where  $C$  represents a capacitance of the island **26**. In other words, a first electron **32** that is introduced onto the island **26** will occupy an allowed state having a potential energy that is greater than that of the conduction band edge  $E_C$  for the material forming the island **26** by  $q^2/2C$ .

A third condition is that, for the electron or electrons **32** to be trapped on the island **26**, the electron charging energy  $q^2/2C$  must be substantially greater than an average thermal energy  $kT$ , or  $q^2/2C > kT$ , where  $k$  represents Boltzmann's constant and  $T$  represents temperature in Kelvin. The capacitance  $C$  must be on the order of one attoFarad for electrons **32** to be trapped on the island **26** for any appreciable length of time at room temperature ( $kT=0.026$  eV at room temperature). For example, an island **26** having a capacitance of  $10^{-16}$  F is about 100 nanometers in diameter but can only exhibit single-electron effects at temperatures at or below about 4 Kelvin. Islands **26** having diameters of one to five nanometers exhibit significant single-electron effects at room temperature (circa 300 K).

FIG. 1B is a simplified potential energy diagram for the device **20** of FIG. 1A showing a potential well **40**, in accordance with the prior art. FIG. 1B shows Fermi levels ("E<sub>F</sub>") **42**, **44** in the first **22** and second **24** electrodes, respectively, a lowest allowed state **46** for one electron **32** in the potential well **40** on the island **26**, and energy barriers **48**, **48'** associated with insulating materials forming the gaps **28**, **28'**, respectively. An important property of the device **20** of FIG. 1A is that no significant current can flow through the device **20** until a magnitude of the potential  $V$  due to the external source **34** equals or exceeds the electron charging energy or  $V \cong q^2/2C$ . FIG. 1C is a simplified potential energy diagram illustrating the potential  $V$  setting the Fermi level **42** at the left side of the Figure equal to the lowest allowed state of the potential well **40**, i.e., at the onset of conduction, in accordance with the prior art.

FIG. 1D is a simplified graph of an I-V characteristic **50** for the device **20** of FIG. 1A, in accordance with the prior

art. The I-V characteristic **50** shows essentially no conduction until the applied voltage  $V$  reaches a threshold  $V_C$ , causing the Fermi level **42** on the electron supply side to be equal to the electron charging energy  $q^2/2C$ . The region of essentially no conduction is known as the Coulomb blockade region. When the applied voltage  $V$  reaches the threshold  $V_C$ , known as the Coulomb gap voltage, the energy barrier effectively vanishes. Linear I-V dependence is seen in FIG. 1D for voltages having an absolute magnitude exceeding  $V_C$ .

FIG. 2 is a simplified schematic illustration of a typical field effect transistor ("FET") **60** that includes the island **26** of FIG. 1A for storing one or more electrons **32**, in accordance with the prior art. The FET **60** includes all of the elements of the two-terminal device **20** of FIG. 1 and additionally includes a gate **62** having a capacitance  $C_G$  and a gate bias supply **64**. The gate bias supply **64** includes a first electrode coupled to the gate **62** and a second electrode coupled to one side of the supply **34** providing the voltage  $V$ . The FET **60** has a channel **66** formed from semiconductor material that is coupled to the first **22** and second **24** electrodes.

Several examples of FETs **60** capable of providing repeatable output signals indicative of single electron **32** storage on the islands **26** are described in "A Room-Temperature Silicon Single-Electron Metal-Oxide-Semiconductor Memory With Nanoscale Floating-Gate and Ultranarrow Channel" by L. Guo et al., *Appl. Phys. Lett.* 70(7) (Feb. 17, 1997), pp. 850-852 and "Fabrication And Characterization of Room Temperature Silicon Single Electron Memory" by L. Guo et al., *J. Vac. Sci. Technol. B* 15(6) (November/December 1997), pp. 2840-2843. Similar FETs **60** are described in "Room Temperature Operation of Si Single-Electron-Memory with Self-Aligned Floating Dot Gate" (IEDM 1996), pp. 952-954; *Appl. Phys. Lett.* 70(13) (Mar. 31, 1997), pp. 1742-1744 and "Si Single Electron Tunneling Transistor With Nanoscale Floating Dot Stacked on a Coulomb Island by Self-Aligned Process", *Appl. Phys. Lett.* 71(3) (Jul. 21, 1997), pp. 353-355, all by A. Nakajima et al. These FETs **60** employ feature sizes as small as 30 nanometers and require much closer alignment between elements than 30 nanometers. Formation of such small feature sizes using electron beam lithography does not presently lend itself to mass production.

These FETs **60** employ a floating island **26** between the gate **62** and the channel **66** to modulate conductivity in the channel **66**. In these FETs **60**, the island **26** spans the width of the channel **66**.

It will be appreciated that other techniques for forming the islands **26** may be employed. For example, shallow implantation of relatively high doses (e.g., ca.  $5-50 \times 10^{14}/\text{cm}^2$ ) of silicon or germanium at relatively low energies (e.g., ca. 20 keV) into relatively thin (e.g., ca. 5-20 or more nanometers) silicon dioxide layers, followed by annealing, provides islands **26** formed from nanocrystals of the implanted species that are insulated from each other and from an underlying silicon region, as described in "Fast and Long Retention-Time Nano-Crystal Memory" by H. Hanafi et al., *IEEE Trans. El. Dev.*, Vol. 43, No. 9 (September 1996), pp. 1553-1558. Performance of memories using islands **36** formed from nanocrystals in proximity to the channel **66** as discussed in "Single Charge and Confinement Effects in Nano-Crystal Memories" by S. Tiwari et al., *Appl. Phys. Lett.* 69(9) (Aug. 26, 1996), pp. 1232-1234.

Prior art FETs may provide multiple islands **26** between the gate **62** and the channel **66**, and are capable of storing

multiple electrons **32**. As a result, these FETs are analogous to conventional flash memories and are capable of multilevel signal storage and readout. An example of an arrangement for discriminating between multiple signal levels that may represent a stored signal is given in "Novel Level-Identifying Circuit for Multilevel Memories" by D. Montanari et al., *IEEE Jour. Sol. St. Cir.*, Vol. 33, No. 7 (July 1998), pp. 1090-1095.

FETs **60** including one or more islands **26** suitable for capture of electrons **32** thus are able to provide measurable and repeatable changes in their electrical properties in response to capture of the electron or electrons **32** on at least one island **26**. Moreover, these FETs **60** provide these changes in a convergent manner, i.e., the changes may be produced by storage of a single electron **32**. In this way, some of the FETs **60** avoid some problems due to number fluctuations in the population of electrons **32** that could otherwise be troublesome for FETs **60** having very small populations of electrons **32**.

Additionally, the energy barriers **48**, **48'** cause the single electron device **20** and the FETs **60** to store trapped electrons **32** for significant periods of time, even in the absence of externally applied electrical power (e.g., voltage sources **34**, **64**). As a result, a nonvolatile memory function is provided by these devices **20** and FETs **60**.

While single electron devices **20** and FETs **60** show great promise as memory cells for very high density memory arrays, fabrication difficulties prevent mass production of memory arrays using these devices **20**, **60** as memory cells. Difficulties in regulating the size of the island or islands **26** and the thickness of the surrounding dielectric materials forming the gaps **28**, **28'** cause problems, particularly with respect to uniformity of device characteristics across many similar devices of a wafer or substrate. Difficulties in realizing the fine line interconnections (e.g., ca. 0.4 micron pitch) and other needed elements also cause poor yields in fabrication of these devices **20**, **60**.

There is therefore a need for a method for fabricating single electron devices that is robust and that provides reproducible single-electron device characteristics.

#### SUMMARY OF THE INVENTION

In one aspect, the present invention includes a memory cell including a MOSFET having a source coupled to a first end of a channel of semiconductor material, a drain coupled to a second end of the channel, a gate formed on a gate insulator on the channel and extending from the source to the drain and a plurality of islands of conductive material having a maximum dimension of three nanometers and surrounded by an insulator having a thickness of between five and twenty nanometers. Each island and surrounding insulator is formed in a pore extending into the channel. As a result, electrons may tunnel into or out of the islands with the assistance of electrical fields resulting from signals coupled to the gate, source and drain. The capacitance of the islands is small enough that single electrons stored on the islands provide externally observable changes in the memory cells.

In other aspects, the present invention provides methods for reading data from, writing data to and erasing memory cells capable of storing data by the presence or absence of a single electron in an island of conductive material contained in the memory cells. The reading, writing and erasing operations may be accompanied by a verification process that compensates for stored charge, trap generation and the like that otherwise might obscure desired data.

#### BRIEF DESCRIPTION OF THE DRAWINGS

FIG. 1A is a simplified schematic diagram of a typical two-terminal single electron device, in accordance with the prior art.

FIG. 1B is a simplified potential energy diagram for the device of FIG. 1A, in accordance with the prior art.

FIG. 1C is a simplified potential energy diagram, illustrating the potential  $V$  setting the Fermi level at the left side of the Figure equal to the lowest allowed state of the potential well of FIG. 1B, in accordance with the prior art.

FIG. 1D is a simplified graph of an I-V characteristic for the device of FIG. 1A, in accordance with the prior art.

FIG. 2 is a simplified schematic illustration of a typical field effect transistor that includes the island of FIG. 1A for storing one or more electrons, in accordance with the prior art.

FIG. 3A is a simplified plan view of a memory device including memory cells employing single electron memory devices having electrical characteristics similar to those of the devices of FIGS. 1 and 2, in accordance with embodiments of the present invention.

FIG. 3B is a simplified isometric view of a single electron MOSFET memory device in the memory cell of FIG. 3A, in accordance with embodiments of the present invention.

FIG. 3C is a simplified cross-sectional view of the device of FIG. 3B, showing islands included within the semiconductor material of the body, in accordance with embodiments of the present invention.

FIG. 4 is a simplified flow chart of a process for reading the memory cell of FIGS. 3A-C, in accordance with embodiments of the present invention.

FIGS. 5 and 6 are simplified flow charts for processes for writing data to the memory cell of FIGS. 3A-C and for erasing data stored in the memory cell, respectively, in accordance with embodiments of the present invention.

FIG. 7 is a graph representing storage and erase time estimates for various energy barriers, in accordance with embodiments of the present invention.

FIG. 8 is a simplified flowchart of a process for forming the islands of FIGS. 1 and 2, in accordance with embodiments of the present invention.

FIGS. 9A-9E are simplified cross-sectional views of the islands as they are being formed using the process of FIG. 8, in accordance with embodiments of the present invention.

FIG. 10 is a simplified block diagram of a computer system including the memory device of FIGS. 3A-C, in accordance with embodiments of the present invention.

#### DETAILED DESCRIPTION OF THE INVENTION

FIG. 3A is a simplified plan view of a memory device 72 including a memory cell 73 having electrical characteristics similar to those of the devices 20 and 60 of FIGS. 1 and 2, in accordance with embodiments of the present invention. The memory device 72 includes a column addressing circuit 74 coupled to a plurality of row address lines 77. The memory cell 73 is located at an intersection of a column address line 75 and a row address line 77 and is addressed by activation of the column 75 and row 77 address lines coupled to the memory cell 73, as is discussed below in more detail.

FIG. 3B is a simplified isometric view of a single electron MOSFET memory device 80 in the memory cell 73 of FIG. 3A, in accordance with embodiments of the present invention. The MOSFET 80 includes a body 82 having a first 84 and second 86 electrodes formed at opposing ends. In one embodiment, the first 84 and second 86 electrodes form low resistance contacts to the body 82. The first electrode 84 is

coupled to a row address line 77 and acts as a drain for the MOSFET 80. The second electrode 86 is coupled to a column address line 75 and acts as a source for the MOSFET 80. In one embodiment, the body 82 includes p-type semiconductor material having an acceptor concentration of about  $10^{15}/\text{cm}^3$  or less and the first 84 and second 86 electrodes are N= contacts to the body 82.

The MOSFET 80 includes a gate 88 coupled to a gate address line 90 for storing data in, and erasing data stored in, the MOSFET 80, and for regulating current through the MOSFET 80. The MOSFET 80 also optionally includes a backgate 88' coupled to a backgate address line 90' for regulating current through the MOSFET 80, and for optionally assisting in data storage and erasure. In one embodiment, the gate 88 and backgate 88' are formed from polysilicon using conventional processing techniques.

FIG. 3C is a simplified cross-sectional view of the MOSFET 80 of FIG. 3B, showing islands 26 (see FIGS. 1 and 2) included within semiconductor material 98 forming the body 82 of the MOSFET 80, in accordance with the embodiments of the present invention. Each island 26 is surrounded by a dielectric 100 that provides the energy barriers 48, 48' (FIGS. 1B and C) associated with the gaps 28, 28', which insulate the island 26 from other islands 26 and from the semiconductor material 98. The gate 88 is biased to be more positive than the second electrode 86, creating a channel 99 extending from the second electrode 86 to the first electrode 84.

The MOSFET 80 of FIGS. 3A-C has a first state exhibiting a first current-voltage characteristic when no electrons 32 are stored on the islands 26 within the MOSFET 80. The MOSFET 80 has a second state exhibiting a second current-voltage characteristic when one or more electrons 32 are stored in one or more islands 26 contained in the body 82 of the MOSFET 80. In the second state, less current passes between the first electrode 84 and the second 86 electrode for a given voltage difference between the first 84 and second 86 electrodes than in the first state, and this difference may be detected by sensing circuitry (not illustrated) coupled to the column 75 or the row 77 address lines. Processes for switching the MOSFET 80 between the first and second states by storage and removal of electrons 32 from the island or islands in the body 82 of the MOSFET 80 are explained in more detail below.

To store one or more electrons 32 in the body 82 of the MOSFET 80, the column address line 75 is coupled to a first voltage (e.g., ground) and the row address line 77 is coupled to a second voltage (e.g., four volts) sufficient to cause single electrons 32 (FIG. 1) to tunnel into and to be stored on one or more of the islands 26 in the body of 82 of the MOSFET 80, as is explained below in more detail with reference to FIG. 5. As a result, the MOSFET 80 changes from the first state to the second state.

To erase information represented by one or more stored electrons 32 stored on the island or islands 26 within the body 82 of the MOSFET 80, the row 77 or column 75 (or both) address line is coupled to an electron sink (e.g., ground). A negative potential is applied to the gate 88 sufficient to completely deplete the semiconductor material 98 forming the body 82 of mobile charge carriers (i.e., electrons 32 or holes) and to tilt the energy barriers 48, 48' (FIG. 1) of the islands 26 to allow any stored electrons 32 to tunnel out of the island or islands 26. Electrons 32 tunneling out of the islands 26 are removed from the semiconductor material 98 by electrical fields induced by a negative voltage applied to the gate electrode 88. A positive

voltage may be applied to the backgate electrode **88'** to aid erasure. As a result, the MOSFET **80** is restored to the first state.

A change in a current  $I_{DS}$  between the first **84** and the second **86** electrode, corresponding to a difference  $\Delta I_{DS}$  in the current  $I_{DS}$  between the first and second states, can be estimated as follows. A total charge  $Q_T$  stored on the islands **26** divided by a gate capacitance  $C_G$  for the MOSFET **80** equals a change in threshold voltage  $\Delta V_T$  for the MOSFET **80**, or  $\Delta V_T = Q_T / C_G$ . For a MOSFET **80** having a gate insulator 10 nanometers thick, a gate length  $L$  of  $10^{-4}$  cm and a gate width  $W$  of  $10^{-4}$  cm, the gate capacitance  $C_G$  is about 3.3 femtoFarad. The change in threshold voltage corresponding to a single electron stored on one of the islands **26** is thus 0.05 millivolts. The drain-source current  $I_{DS}$  is given as  $I_{DS} = \mu C_G (W/L) (V_{GS} - V_T)^2 / 2$ , where  $V_{GS}$  represents the voltage between the gate **88** and the source **86** for the MOSFET **80** and  $\mu$  represents the electron mobility. An estimate for a change in the drain-source current  $\Delta I_{DS}$  due to a change in threshold voltage  $\Delta V_T$  is  $\Delta I_{DS} = \mu C_G (W/L) (V_{GS} - V_T) \Delta V_T$ . For this example, a mobility of  $\mu$  of 600  $\text{cm}^2/(\text{v}\cdot\text{sec})$  and voltage difference  $V_{GS} - V_T$  of two volts corresponds to a decrease in current  $\Delta I$  due to one stored electron **32** of 10 nanoamperes.

In one embodiment, the body **82** of the MOSFET **80** may have a length  $L$  of about one micrometer ( $10^{-4}$  cm), a cross-sectional area  $A$  of about  $10^{-8}$   $\text{cm}^2$  and a thickness of the body **82** of about one micrometer. A free carrier concentration  $10^{15}/\text{cm}^3$  or less allows the gate **88** and the backgate **88'** to be able to deplete the semiconductor material **98** with relatively low applied voltages.

FIG. **4** is a simplified flow chart of a process **120** for reading the memory cell **73** of FIG. **3A**, in accordance with embodiments of the present invention. The process **120** begins in a step **122** by activating one of the column address lines **75** and one of the row address lines **77** of FIGS. **3A-C** to address one of the memory cells **73**, and is discussed below in more detail. In a step **124**, a bias current  $I_B$  or voltage  $V_B$  is applied to the addressed memory cell **73**. In a step **126**, the addressed memory cell **73** is coupled to a sensing circuit (not shown). In some embodiments, a query task **128** then compares a measured response  $X_M$  to a threshold  $X_T$  to determine if a logical "1" or a logical "0" is stored in the memory cell **73** as is described below in more detail.

In one embodiment, when a bias current  $I_B$  is supplied from a current source (not shown) to, for example, the first electrode **84** of the addressed memory cell **73**, the measured response  $X_M$  is a voltage, such as a drain-source voltage, measured across the first **84** and second **86** electrodes. When, for example, the query task **128** determines that the measured response  $X_M$  exceeds the threshold  $X_T$ , at least one electron **32** is stored in the memory cell **73** and the memory cell **73** is storing a first logical state. When the query task **128** determines that the measured response  $X_M$  does not exceed the threshold  $X_T$ , no electron **32** is stored in the memory cell **73** and the memory cell **73** is storing a second logical state.

Conversely, in another embodiment, when a bias voltage  $V_B$  is supplied from a voltage source (not shown) to, for example, the gate **88** of the addressed memory cell **73**; the measured response  $X_M$  exceeds the threshold  $X_T$ , no electron **32** is stored in the memory cell **73** and the memory cell **73** is in the second logical state. When the query task **128** determines that the measured response  $X_M$  does not exceed the threshold  $X_T$ , at least one electron **32** is stored in the memory cell **73** and the memory cell **73** is in the first logical state.

When the query task **128** determines that the memory cell **73** is in the first logical state, the comparison circuit indicates that the memory cell **73** is in the first logical state, e.g., that a logical "1" is stored in the memory cell **73**, in a step **130**. When the query task **128** determines that the memory cell **73** is in the second logical state, the comparison circuit indicates that a logical "0" is stored in the memory cell **73** in a step **132**. The process **120** ends following either step **130** or step **132**.

In another embodiment, the query task **128** discriminates between a plurality of different logical values or states that may be stored in the memory cell **73** by comparing the measured response  $X_M$  to a plurality of thresholds  $X_T$ . An example of an arrangement for discriminating between multiple signal levels that may represent a stored signal is given in "Novel Level-Identifying Circuit for Multilevel Memories" by D. Montanari et al., IEEE Jour. Sol. St. Cir., Vol. 33, No. 7 (July 1998), pp. 1090-1095. An example of a circuit and method for programming, reading and erasing multiple single electron differences in the FETs **80** of FIGS. **3A-C** is given in "Multi-State Flash Memory Cell and Method for Programming Single Electron Differences" by L. Forbes, U.S. Pat. No. 5,740,104. After the query task **128** determines the correct logical value for the data stored in the memory cell **73**, the data comparison circuit indicates the correct logical value in the steps **130-132** and the process **120** ends.

FIGS. **5** and **6** are simplified flow charts for processes **140** and **160** for writing data to the memory cell **73** of FIG. **3A** and for erasing data stored in the memory cell **73**, respectively, in accordance with embodiments of the present invention. The processes **140** and **160** both use a verification process similar to a conventional verification process used with flash memories to compensate for variations in memory cell characteristics from one memory cell **73** to another, as described in "Verify: Key to the Stable Single-Electron-Memory Option" by T. Ishii et al. (1979 IEDM), pp. 171-174.

With reference now to FIG. **5**, the write process **140** begins in a step **142** by activating one of the column address lines **75** and one of the row address lines **77** of FIGS. **3A-C** to address one of the memory cells **73**. In a step **144**, a write pulse, which may be either a current  $I_W$  or a voltage  $V_W$  pulse, is applied to the addressed memory cell **73**. In some embodiments, the step **144** is used to write a binary value to the memory cell **73**. In other embodiments, the step **144** is used to write one of a plurality of possible values or data entries to the memory cell **73** by injecting a controlled number of electrons **32** into the islands **26** of the memory cell **73**.

In a step **146**, an index variable  $n$ , corresponding to a number of write cycles applied to this memory cell during this write process **140**, is incremented. In a step **148**, the memory cell **73** is read by sampling a voltage or current associated with the memory cell **73**. A query task **150** then compares the read data to the data written to the memory cell **73** in the step **144**.

When the query task **150** determines that the read data and the write data agree, the process **140** ends. When the query task **150** determines that the read data and the write data do not agree, control passes to a query task **152** to determine if a maximum number of cycles  $N$  has been reached (i.e., is  $n \geq N$ ?). The maximum number of cycles  $N$  is chosen to allow all working memory cells **73** to be programmed, despite differences in programming time between cells **73**, without wasting excessive amounts of time in attempts to

program defective memory cells **73**. When the query task **152** determines that the maximum number of cycles **N** has not been reached, control passes to the step **144**, and steps **144–150** or **152** repeat. When the query task **152** determines that the maximum number of cycles **N** has been reached, a step **154** records that a write failure has occurred and the process **140** ends.

In some embodiments, the record of a write failure that is generated in the step **154** may be used to construct a conventional memory map describing addresses of defective memory cells **73**. Memory maps are used in order to avoid writing data to, or attempting to write data to, or reading data from, memory cells **73** that are defective. In some embodiments, the record of a write failure that is generated in the step **154** may be used to replace defective memory cells **73** with memory cells **73** that are known to be working properly, as is conventional in fabrication and repair of memory devices such as dynamic random access memories.

In the step **144**, where a write pulse is applied to the memory cell **73**, a finite number of electrons **32** are injected into the island or islands **26**. A probability of write failure is finite and nonzero because injection of electrons **32** into the potential wells **40** (FIG. **1C**) is essentially stochastic. For example, a failure probability of 0.1% is unacceptable in modern memory devices. Additionally, characteristics of the memory cell **73** may change with time, due to generation of new trapping centers or by trapping of charge in or near the memory cell **73**.

Reading data from the memory cell **73** after a write pulse has been applied to the memory cell allows determination that a write failure has occurred. By making the write pulse  $I_w$  or  $V_w$  longer as  $n$  increases, the probability of trapping the desired number of electrons **32** increases substantially and may approach unity. In one embodiment, a width  $W_w$  of the write pulses  $I_w$  or  $V_w$  depends geometrically on  $n$ , e.g.,  $W_w(n)2^n$ ,  $n \in \{1\}$ . In another embodiment, the amplitude of the write pulses depends arithmetically on  $n$ , e.g.,  $V_w(n) V_w(0)(1 \times n/M)$ ,  $n \in \{1\}$ , where  $V_w(0)$  represents an initial value and  $M$  represents a proportionality constant.

With reference now to FIG. **6**, the erase process **160** begins in a step **162** by activating one or more of the column address lines **75** and one or more of the row address lines **77** of FIGS. **3A–C** to address one or more of the memory cells **73**. In one embodiment, the step **162** selects a group of memory cells **73**, which may be a subset of the memory cells on one memory device **72**, may be all of the memory cells **73** on a memory device **72** or may include memory cells **73** from more than one memory device **72**. In a step **164**, an erase voltage pulse  $V_E$  is applied to the addressed memory cell **73**. In one embodiment, the erase pulse includes a negative voltage pulse applied to the gate **88**. A positive erase pulse may also be applied to the optional backgate **88'**. In a step **166**, an index variable  $n$ , corresponding to a number of erase cycles applied to this memory cell **80** during this erase process **160**, is incremented. In a step **168**, the memory cell **73** is read by sampling a voltage or current associated with the memory cell **73**. A query task **170** then compares the read data to an expected value (e.g., corresponding to an absence of stored electrons **32**) to determine if the contents of the memory cell **73** were erased in the step **164**.

When the query task **170** determines that the contents of the memory cell **73** are erased, the process **160** ends. When the query task **170** determines that the contents of the memory cell **73** are not erased, control passes to a query task **172** to determine if a maximum number of cycles **N** has been reached (i.e., is  $n \geq N$ ?). As with the write process **140** of

FIG. **5**, **N** is chosen to balance differences in erase time from one memory cell **73** to another cell **73** without spending excessive time to erase defective memory cells **73**. When the query task **172** determines that the maximum number of cycles **N** has not been reached, control passes back to the step **164**, and steps **164–170** or **172** repeat. In accordance with embodiments of the invention, the erase pulses  $V_E$  may be varied with  $n$  as described above for the write pulses  $I_w$  or  $V_w$  in connection with the process **140** of FIG. **5**. When the query task **172** determines that the maximum number of cycles **N** has been reached, a step **174** records that an erase failure has occurred. The process then **160** ends.

In one embodiment, individual memory cells **73** are erased as needed for storage of new data. In another embodiment, all of the memory cells **73** in a group or in an entire memory device **72** are erased en masse, by addressing a group of memory cells **73** in the step **162** and application of the erase pulses in the step **164** to all of the memory cells **73** in the group or in the memory device **72** simultaneously. The steps **166–174** are then carried out for each memory cell **73** individually, with a step of addressing the individual memory cells **73** being carried out prior to the step **166** of incrementing the index variable  $n$ . In another embodiment, the memory cells are erased en masse, however, the steps **166–174** are carried out as steps **146–154** of the verified write process **140** of FIG. **5**.

An advantage of en masse erasure is that the erase process **160** is slow, typically requiring milliseconds. Erasure of the entire memory device **72** one memory cell **73** at a time takes much longer than erasure of the entire memory device **72** en masse, and this is more exaggerated as the number of memory cells **73** in the memory device **72** increases.

Several factors affect storage times  $\tau_s$ , also known as latency, for memory cells **73** incorporating islands **26** for storage of one or more electrons **32**. In general,  $\tau_s e^{(\Delta E/kT)}$ , where  $\Delta E$  represents the energy level difference between the energy barriers **48**, **48'** and the lowest allowed state in the island **26** and  $d/d_0$  represents a normalized thickness of gaps **28**, **28'**. Larger  $\Delta E$  values or large  $d/d_0$  values provide for longer storage times but also require higher write and erase pulse magnitudes and greater pulse durations. Additionally,  $\Delta E$  is a function of the material forming the island **26** and the material forming the gaps **28**, **28'**. The energy level difference  $\Delta E$  may be estimated by subtracting the electron affinity  $\chi_{MNS}$  for the material forming the gaps **28**, **28'** from the electron affinity  $\chi_{ISL}$  for the material making up the island **26** and then adding the electron charging energy  $q^2/2C$ , i.e.,  $\Delta E = \chi_{ISL} - \chi_{MNS} + q^2/2C$ . Representative values for electron affinities  $\chi$  for several materials are summarized below in Table I. Measured or achieved electron affinities  $\chi$  depend strongly on surface treatment and surface contamination and may vary from the values given in Table I.

TABLE I

Electron affinities $\chi$ for selected materials		
$\chi$ (eV)	Material	Use
4.05	Si	Islands
3.6/3.7*	SiC	Islands
1.4**	C (diamond)	Islands

TABLE I-continued

Electron affinities $\chi$ for selected materials		
$\chi$ (eV)	Material	Use
0.9–4.05	Silicon oxycarbide (projected)	Islands
0.9	SiO <sub>2</sub>	Gaps

\*depending on surface treatment

\*\*diamond can manifest different values, including negative values.

FIG. 7 is a graph representing estimated storage **176** and erase **178** time estimates for various island electron affinities  $\chi_{ISL}$  together with SiO<sub>2</sub> barriers in accordance with embodiments of the present invention. The left ordinates correspond to a logarithm of retention time **176** at constant temperature, while the right ordinates correspond to a logarithm of erase time **178** at constant erase voltage. Erase times **178** for the memory device **72** are determined in part by the height of the energy barrier **48**, **48'** (FIGS. 1B and C) surrounding the island **26**.

Lower energy barriers **48**, **48'** provide shorter tunneling distances and much higher tunneling probabilities. Short erase times **178** are desirable for some applications of electronically-erasable memories such as the memory device **72**.

Lower barriers **48**, **48'** also result in shorter retention times **176** due to thermal activation of electrons **32** over or through the energy barriers **48**, **48'**. The islands **26** may be formed from silicon, from microcrystalline diamond-like films of Si<sub>(1-x)C<sub>x</sub></sub>, with the composition ratio, x, ranging from 0.5 to one, or from silicon oxycarbide compounds, to provide electron affinities  $\chi$  ranging between about 4.05 eV and 0.9 eV or less (see Table I), corresponding to energy barriers  $\Delta E$  ranging from about 3.95 to about 0 eV (ignoring the charging voltage). By changing the composition of the islands **26** and the thickness of the surrounding insulator, and thus the height of the energy barriers **48**, **48'**, charge retention times **176** can be changed from seconds, characteristic of DRAMs, to years, characteristic of hard disk drives. As a result, the memory device **72** can either be made to emulate a DRAM or a hard disk drive by varying the composition of the islands **26**. One device type can then perform all memory functions.

FIG. 7 illustrates that storage **176** and erase **178** times vary exponentially with the height of the energy barriers **48**, **48'**. Presently, memories using polycrystalline silicon floating gates embedded in silicon dioxide are estimated to have charge retention times **176** of millions of years at 85° C. because the energy barriers **48**, **48'** may result in reliability problems or, in the worse case, lead to breakdown and catastrophic failure of the device **72**. An island **26** may be composed of a material of lower or adjusted barrier height, such as diamond-like compounds of silicon, carbon and oxygen, to provide desired energy barriers **48**, **48'**. As a result, an acceptable retention time **176** can be established, whether seconds or years, by varying the relative concentrations of Si, C and O, thereby varying the electron affinity  $\chi$  for the islands **26**. This then determines the height of the energy barriers **48**, **48'** and therefore, in part, the erase time **178** for a particular erase voltage.

FIG. 7 shows the concepts involved using rough order-of-magnitude estimates of the variations of storage **176** and erasure **178** times with barrier height  $\Delta E$ . The same device structure can be used either as replacements for DRAMS or as replacements for hard disk drives. Only the composition of the island **26** needs to be changed in order to change the

retention time **176** and the erasure characteristics **178**. This may be done on one integrated circuit so that radically different types of memory functions are realized on one integrated circuit.

FIG. 8 is a simplified flowchart of a process **180** for forming the islands **26** of FIGS. 1 and 2, and FIGS. 9A–9E are simplified cross-sectional views of the islands **26** as they are being formed using the process **180** of FIG. 8, in accordance with embodiments of the present invention. The process **180** (FIG. 8) begins in a step **182** with formation of voids or pores **202** (FIG. 9A) in a suitable silicon substrate or layer **98** (FIGS. 3C and 9A–9E). In one embodiment, the voids or pores **202** are formed by processes similar to those described in “On the Morphology of Porous Silicon Layers Obtained by Electrochemical Method” by G. Graciu et al., International Semiconductor Conference CAS '95 Proceedings (IEEE Catalog No. 95TH8071) (1995), pp. 331–334. In one embodiment, a current density of between 1.5 and 30 mA/cm<sup>2</sup> is employed together with either 36 weight % HF-ethanol 1:1 or 49 weight % HF-ethanol 1:3. Pores **202** are to have the desired characteristics readily and uniformly formed using simple and easily controlled processes.

In a step **184**, the silicon **98** including interiors of the pores **202** is oxidized to provide a thin oxide layer **100** (FIG. 8). In one embodiment, the silicon **98** is oxidized to provide the oxide layer **100** to have a thickness of between 2.5 and ten nanometers. The step **184** may be carried out using conventional oxidation techniques. In one embodiment, an inductively-coupled oxygen-argon mixed plasma is employed for oxidizing the silicon **98**, as described in “Low-Temperature Si Oxidation Using Inductively Coupled Oxygen-Argon Mixed Plasma” by M. Tabakomori et al., Jap. Jour. Appl. Phys., Part 1, Vol. 36, No. 9A (September 1997), pp. 5409–5415. In another embodiment, electron cyclotron resonance nitrous oxide plasma is employed for oxidizing the silicon **98**, as described in “Oxidation of Silicon Using Electron Cyclotron Resonance Nitrous Oxide Plasma and its Application to Polycrystalline Silicon Thin Film Transistors”, J. Lee et al., Jour. Electrochem. Soc., Vol. 144, No. 9 (September 1997), pp. 3283–3287 and “Highly Reliable Polysilicon Oxide Grown by Electron Cyclotron Resonance Nitrous Oxide Plasma” by N. Lee et al., IEEE El. Dev. Lett., Vol. 18, No. 10 (October 1997), pp. 486–488.

In a step **186**, a conductive material **204** is formed over the surface of the silicon **98** and in the pores **202**. In some embodiments, semiconductor material **204** (FIG. 9C) is formed over the surface of the silicon **98** and in the pores **202**.

Examples of materials **204** that may be used in accordance with embodiments of the invention include the materials listed in Table I above. The material **204** within the pores **202** forms the islands **26** and is chosen to have an electron affinity  $\chi$  that, together with the thickness  $d/d_0$  and the electron affinity  $\chi$  of insulator **100** filling the gaps **28**, **28'** (FIGS. 1A and 2), provides storage times in a range of from hours to days or longer, together with practical erase parameters.

In some embodiments, silicon oxycarbide is employed as the material **204** in step **186**. A process for forming thin microcrystalline films of silicon oxycarbide is described in “Transport Properties of Doped Silicon Oxycarbide Microcrystalline Films Produced by Spatial Separation Techniques” by R. Martins et al., Solar Energy Materials and Solar Cells 41/42 (1996), pp. 493–517. A diluent/reaction gas (e.g., hydrogen) is introduced directly into a region where plasma ignition takes place. The mixed gases con-

taining the species to be deposited are introduced close to the region where the growth process takes place, which is often the substrate heater. A bias grid is located between the plasma ignition and the growth regions, spatially separating the plasma and growth regions.

Deposition parameters for producing doped microcrystalline  $\text{Si}_x\text{C}_y\text{O}_z\text{H}$  films may be defined by determining the hydrogen dilution rate and power density that lead to microcrystallization of the grown film **204**. The power density is typically less than 150 milliwatts per  $\text{cm}^2$  for hydrogen dilution rates of 90%+, when the substrate temperature is about 250° C. and the gas flow is about 150 sccm. The composition of the films may then be varied by changing the partial pressure of oxygen during film growth to provide the desired characteristics.

In some embodiments, SiC is employed as the material **204** in the step **186**. SiC films may be fabricated by chemical vapor deposition, sputtering, laser ablation, evaporation, molecular beam epitaxy or ion implantation. Vacuum annealing of silicon substrates is another method that may be used to provide SiC layers having thicknesses ranging from 20 to 30 nanometers, as described in "Localized Epitaxial Growth of Hexagonal and Cubic SiC Films on Si by Vacuum Annealing" by Luo et al., Appl. Phys. Lett. 69(7) (1996), pp. 916-918. Prior to vacuum annealing, the substrates are degreased with acetone and isopropyl alcohol in an ultrasonic bath for fifteen minutes, followed by cleaning in a solution of  $\text{H}_2\text{SO}_4\text{:H}_2\text{O}_2$  (3:1) for fifteen minutes. A five minute rinse in deionized water then precedes etching with a 5% HF solution. The substrates are blown dry using dry nitrogen and placed in a vacuum chamber. The chamber is pumped to a base pressure of  $1-2 \times 10^{-6}$  Torr. The substrate is heated to 750 to 800° C. for half an hour to grow the microcrystalline SiC film.

In some embodiments, silicon is employed as the material **204** in the step **186**. Methods for depositing high quality polycrystalline films of silicon on silicon dioxide substrates are given in "Growth of Polycrystalline Silicon at Low Temperature on Hydrogenated Microcrystalline Silicon ( $\mu\text{-Si:H}$ ) Seed Layer" by Parks et al., Proceedings of the 1997 MRS Spring Symposium, Vol. 467 (1997), pp. 403-408, "Novel Plasma Control Method in PECVD for Preparing Microcrystalline Silicon" by Nishimiya et al., Proceedings of the 1997 MRS Spring Symposium, Vol. 467 (1997), pp. 397-401 and "Low Temperature (450° C.) Poly-Si Thin Film Deposition on  $\text{SiO}_2$  and Glass Using a Microcrystalline-Si Seed Layer" by D. M. Wolfe et al., Proceedings of the 1997 MRS Spring Symposium, Vol. 472 (1997), pp. 427-432. A process providing grain sizes of about 4 nm is described in "Amorphous and Microcrystalline Silicon Deposited by Low-Power Electron-Cyclotron Resonance Plasma-Enhanced Chemical-Vapor Deposition" by J. P. Conde et al., Jap. Jour. Of Appl. Phys., Part I, Vol. 36, No. 1A (June 1997), pp. 38-49. Deposition conditions favoring small grain sizes for microcrystalline silicon include high hydrogen dilution, low temperature, low deposition pressure and low source-to-substrate separation.

In a step **188**, the portion of the materials **204** deposited in the step **186** that are located on the surface of the silicon body **98** are effectively removed. In one embodiment, in the step **188**, the portion of the materials **204** that are located on the surface of the silicon **98** are oxidized to provide a structure as illustrated in FIG. **9D**. The step **188** proceeds until the material **204** on the surface is completely oxidized but does not proceed for long enough to oxidize all of the material **204** surrounded by silicon dioxide **100** are formed in the pores **202** in the single crystal silicon **98** forming the body **82** of the MOSFET **80** (FIGS. **3A-C**).

Significantly, the materials listed in Table I for use in the islands **26** can be oxidized to form silicon dioxide **208** or to form a volatile gas ( $\text{CO}_2$ ). As a result, the islands **26** may be isolated from each other by a simple oxidation process that may not require a photolithographic step.

In a step **190**, an optical gate oxide **210** (FIG. **9E**) is formed on the surface of the silicon **98** and on top of the material **204** deposited in the pores **202**. In a step **192**, the gate oxide is patterned using conventional techniques. In a step **194**, the gate **88** and backgate **88'** (FIGS. **3B** and **C**) are formed. In one embodiment, the gate **88** and backgate **88'** are conventionally formed from polysilicon. The process **180** then ends and further fabrication is carried out using conventional processing. An advantage of the process **180** is that it does not rely on very-fine-line lithography for formation of the islands **26**.

Approaches using such fine line lithography are described in "A Room-Temperature Silicon Single-Electron Metal-Oxide-Semiconductor Memory With Nanoscale Floating-Gate and Ultranarrow Channel" by L. Guo et al., Appl. Phys. Lett. 70(7) (Feb. 17, 1997), pp. 850-852 and "Fabrication And Characterization of Room Temperature Silicon Single Electron Memory" by L. Guo et al., J. Vac. Sci. Technol. B 15(6) (November/December 1997), pp. 2840-2843. These devices were fabricated using e-beam lithography and incorporate features having widths as narrow as 25 nanometers. Similarly, devices described in "Room Temperature Operation of Si Single-Electron-Memory with Self-Aligned Floating Dot Gate" (IEDM 1996), pp. 952-954, Appl. Phys. Lett. 70(13) (Mar. 31, 1997), pp. 1742-1744 and "Si Single Electron Tunneling Transistor With Nanoscale Floating Dot Stacked on a Coulomb Island by Self-Aligned Process", Appl. Phys. Lett. 71(3) (Jul. 21, 1997), pp. 353-355, all by A. Nakajima et al., employ feature sizes as small as 30 nanometers and require much closer alignment between elements than 30 nanometers. Formation of such small feature sizes using electron beam lithography does not presently lend itself to mass production.

It will be appreciated that other techniques for forming the islands **26** (FIG. **3C**) may be employed. For example, shallow implantation of relatively high doses (e.g., ca.  $5-50 \times 10^{14}/\text{cm}^2$ ) of silicon germanium at relatively low energies (e.g., ca. 20 keV) into relatively thin (e.g., ca. 5-20 or more nanometers) silicon dioxide layers, followed by annealing, provides nanocrystals of the implanted species that are insulated from each other and from an underlying silicon region, as described in "Fast and Long Retention-Time Nono-Crystal Memory" by H. Hanafi et al., IEEE Trans. El. Dev., Vol. 43, No. 9 (Sep. 1996), pp. 1553-1558. Performance of memories using nanocrystals in proximity to a channel is discussed in "Single Charge and Confinement Effects in Nano-Crystal Memories" by S. Tiwari et al., Appl. Phys. Lett. 69(9) (Aug. 26, 1996), pp. 1232-1234.

FIG. **10** is a simplified block diagram of a portion of a computer system **220** including the memory of MOSFET **80** of FIGS. **3A-C**, in accordance with embodiments of the present invention. The computer system **220** includes a central processing unit **222** for performing various computing functions, such as executing specific software to perform specific calculations or tasks. The central processing unit **222** is coupled via a bus **224** to a memory **226**, a user input interface **228**, such as a keyboard or a mouse, and a display **230**. The memory **226** may or may not include a memory management module (not illustrated) and does include ROM for storing instructions providing an operating system and read-write memory for temporary storage of data. The processor **222** operates on data from the memory **226** in

15

response to input data from the user input interface **228** and displays results on the display **230**. The processor **222** also stores data in the read-write portion of the memory **226**. The integrated circuit **72** (FIG. 3A) is particularly useful when it is a memory integrated circuit in the read-write memory portion of the memory **226**, because it may then allow the memory **226** to provide increased information storage capacity and/or density.

The embodiments of the present invention provide a compact, sensitive memory cell and permit very high storage capacity memories to be fabricated. Additionally, the inventive memory cell does not require high resolution lithography for fabrication of the islands that store charge.

It is to be understood that even though various embodiments and advantages of the present invention have been set forth in the foregoing description, the above disclosure is illustrative only, and changes may be made in detail, and yet remain within the broad principles of the invention. Therefore, the present invention is to be limited only by the appended claims.

What is claimed is:

**1.** A method of erasing data from a selected memory cell by including one or more islands of conductive material, each island surrounded by an insulator and extending into a pore anodically formed in a MOSFET channel, comprising: applying a voltage to a gate electrode coupled to the channel; and

providing a return path for current through one of a source and a drain formed on the channel to either side of the gate electrode.

**2.** The method of claim **1** wherein the act of applying a voltage to a gate electrode comprises applying a negative voltage pulse to the gate electrode having a duration and amplitude sufficient to promote field-assisted tunneling of trapped electrons from the islands to the channel.

**3.** The method of claim **1** wherein the act of applying a voltage to a gate electrode comprises applying a positive voltage pulse having a duration and amplitude sufficient to promote field-assisted tunneling of trapped electrons from the islands to the channel and also sufficient to promote tunneling of the electrons through a gate dielectric to the gate electrode.

16

**4.** The method of claim **1**, further comprising:

reading the selected memory cell after applying the voltage to the gate electrode;

comparing a result from reading the selected memory cell to an expected value; and

iterating applying a voltage, providing a return path, reading the selected memory cell and comparing a result from reading the selected memory cell when comparing the read data to the expected value shows disagreement.

**5.** The method of claim **4** wherein the act of iterating includes:

incrementing a count for each iteration;

comparing the count to a maximum number of iterations for each iteration; and

ceasing iterating when the count equals or exceeds the maximum number of iterations.

**6.** The method of claim **4** wherein the act of reading the selected memory cell comprises:

applying a drain current to the MOSFET;

measuring a drain-source voltage across the MOSFET;

comparing the measured voltage to a threshold voltage;

providing an indication of a first logical state when the measured voltage exceeds the threshold; and

providing an indication of a second logical state when the measured voltage does not exceed the threshold.

**7.** The method of claim **4** wherein the act of reading the selected memory cell comprises:

applying a drain-source voltage to the MOSFET;

measuring a drain current through the MOSFET;

comparing the measured current to a threshold current;

providing an indication of a first logical state when the measured current does not exceed the threshold; and

providing an indication of a second logical state when the measured current exceeds the threshold.

\* \* \* \* \*